Funafuti Atoll

Chapter 15
Tuvalu

The contributions of Hilia Vavae and Kilateli Epu from the Tuvalu Meteorological Service are gratefully acknowledged

Introduction

This chapter provides a brief description of Tuvalu, its past and present climate as well as projections for the future. The climate observation network and the availability of atmospheric and oceanic data records are outlined. The annual mean climate, seasonal cycles and the influences of large-scale climate features such as the South Pacific Convergence Zone and patterns of climate variability (e.g. the El Niño-Southern Oscillation) are analysed and discussed. Observed trends and analysis of air temperature, rainfall, extreme events (including tropical cyclones), sea-surface temperature, ocean acidification, mean and extreme sea levels are presented. Projections for air and sea-surface temperature, rainfall, sea level, ocean acidification and extreme events for the 21st century are provided. These projections are presented along with confidence levels based on expert judgement by Pacific Climate Change Science Program (PCCSP) scientists. The chapter concludes with a summary table of projections (Table 15.4). Important background information including an explanation of methods and models is provided in Chapter 1. For definitions of other terms refer to the Glossary.

15.1 Climate Summary

15.1.1 Current Climate

- Tuvalu's climate is characterised by two distinct seasons: a wet season from November to April and a dry season from May to October.
- The strong seasonal cycle is driven by the strength of the South Pacific Convergence Zone, which is strongest during the wet season. The West Pacific Monsoon can also bring high rainfall to Tuvalu during the wet season.
- Air temperatures in Tuvalu are relatively constant throughout the year and are closely related to sea-surface temperatures.
- Warming trends are evident in both annual and seasonal mean air temperatures at Funafuti for the period 1950–2009.
- High year-to-year variability in rainfall is mostly due to the impact of the El Niño-Southern Oscillation.
- Annual and seasonal rainfall trends for Funafuti and Nanumea for the period 1950–2009 are not statistically significant.
- The sea-level rise near Tuvalu measured by satellite altimeters since 1993 is about 5 mm per year.
- On average Funafuti experiences eight tropical cyclones per decade, with most occurring between November and April. The high interannual variability in tropical cyclone numbers makes it difficult to identify any long-term trends in frequency.

15.1.2 Future Climate

Over the course of the 21st century:

- Surface air temperature and sea-surface temperature are projected to continue to increase (*very high* confidence).
- Annual and seasonal mean rainfall is projected to increase (*high* confidence).
- The intensity and frequency of days of extreme heat are projected to increase (*very high* confidence).
- The intensity and frequency of days of extreme rainfall are projected to increase (*high* confidence).
- The incidence of drought is projected to decrease (*moderate* confidence).
- Tropical cyclone numbers are projected to decline in the south-east Pacific Ocean basin (0–40ºS, 170ºE–130ºW) (*moderate* confidence).
- Ocean acidification is projected to continue (*very high* confidence).
- Mean sea-level rise is projected to continue (*very high* confidence).

15.2 Country Description

Tuvalu lies is the western South Pacific Ocean between 176°E–180°E and 5°S–11°S. The country consists of five true atolls and four raised limestone reef islands, with a total land area of approximately 26 km^2. The maximum height of the land above mean sea level typically ranges from three to four metres. The area of the Exclusive Economic Zone is 900 000 km^2.

The capital of Tuvalu, Funafuti, is located on the atoll with the same name (Tuvalu's Pacific Adaptation to Climate Change, 2006). The estimated population of Tuvalu in 2010 was 11 149 (Tuvalu Country Statistics, SOPAC, 2010).

Tuvalu's economy is dominated by subsistence farming and fishing activities. Commercial fishing is an expanding economic activity (Tuvalu's First National Communication under the UNFCCC, 1999).

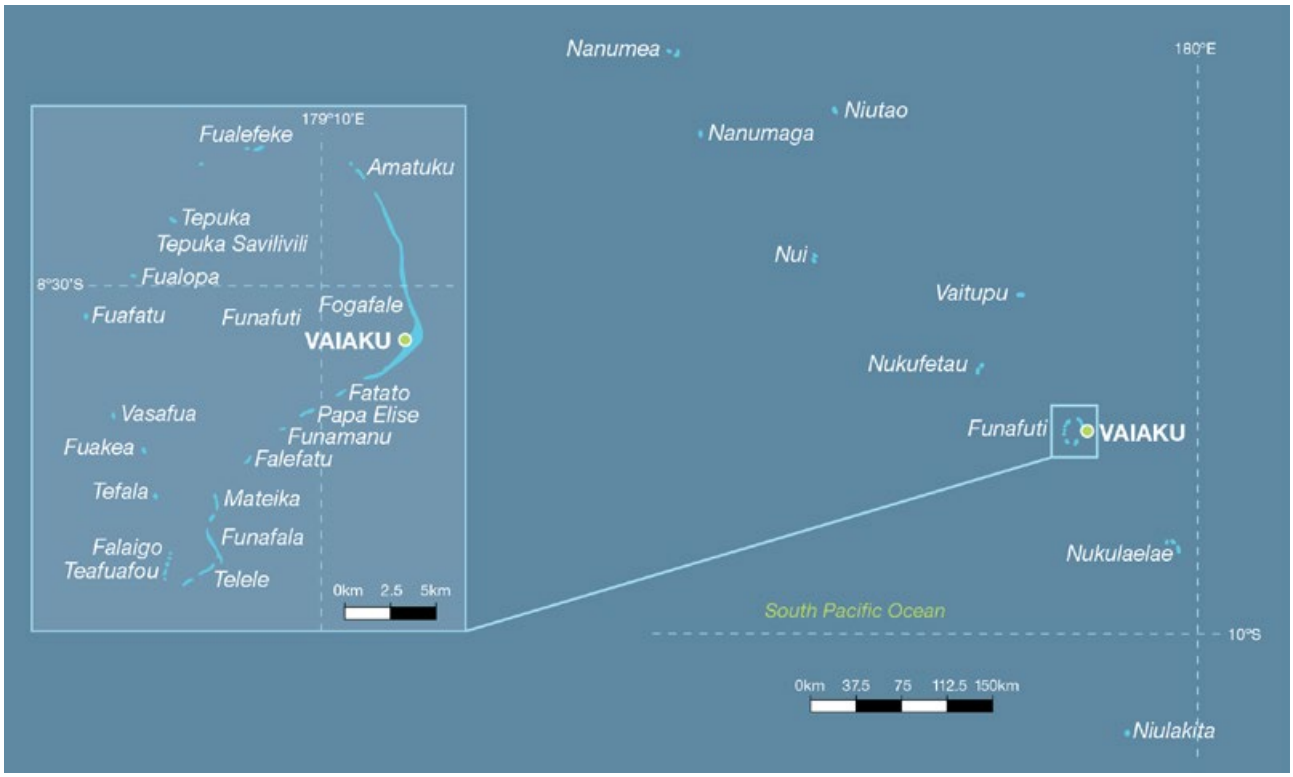

Figure 15.1: Tuvalu

15.3 Data Availability

There are nine operational meteorological stations in Tuvalu at the present time. Multiple observations within a 24-hour period are taken at four stations (Nanumea, Nui, Funafuti and Niulakita) and there are single observation rainfall stations at five locations: Nanumaga, Niutao, Nukufetau, Vaitupu and Nukulaelae. The Funafuti station has the longest record, with rainfall data available from 1927 and air temperature data from 1933.

Climate records for Funafuti and rainfall records for Nanumea for the period 1950–2009 have been used. The Funafuti climate station is located on the Fongafale islet on the eastern side of the Funafuti atoll in southern Tuvalu. Nanumea is the northernmost island in the Tuvalu group (Figure 15.1). Both records are homogeneous and more than 99% complete.

Monthly-averaged sea-level data are available from 1977 at Funafuti (1977–2001 and 1993–present). A global positioning system instrument to estimate vertical land motion was deployed at Funafuti in 2001 and will provide valuable direct estimates of local vertical land motion in future years. Both satellite (from 1993) and in situ sea-level data (1950–2009; termed reconstructed sea level; Volume 1, Section 2.2.2.2) are available on a global 1° x 1° grid.

Long-term locally-monitored sea-surface temperature data are unavailable for Tuvalu, so large-scale gridded sea-surface temperature datasets have been used (HadISST, HadSST2, ERSST and Kaplan Extended SST V2; Volume 1, Table 2.3).

15.4 Seasonal Cycles

Mean annual rainfall in the south of Tuvalu, including Funafuti, is around 3400 mm. Approximately 2900 mm per year falls at Nanumea in the north. The climate of Tuvalu is characterised by two distinct seasons: a wet season from November to April and a dry season from May to October (Figure 15.2). The wet season is shorter in Nanumea. This strong seasonal cycle is driven by the strength of the South Pacific Convergence Zone (SPCZ), which is strongest during the wet season. The West Pacific Monsoon can also bring high rainfall to Tuvalu during the wet season. Rainfall averages more than 200 mm each month of the year in Funafuti and more than 160 mm in Nanumea, reflecting the location of Tuvalu near the West Pacific Warm Pool, where convective rainfall occurs year-round.

Funafuti has virtually no seasonal cycle for maximum and minimum air temperature, with maxima averaging around 31°C and minima 25–26°C, all year round (Figure 15.2). Being on a small atoll island surrounded by ocean, air temperatures in Tuvalu are strongly related to sea-surface temperatures around the islands. Sea-surface temperatures around Nanumea are very similar to those around Funafuti and so air temperatures are similar there, although no long-term air temperature data at Nanumea are available.

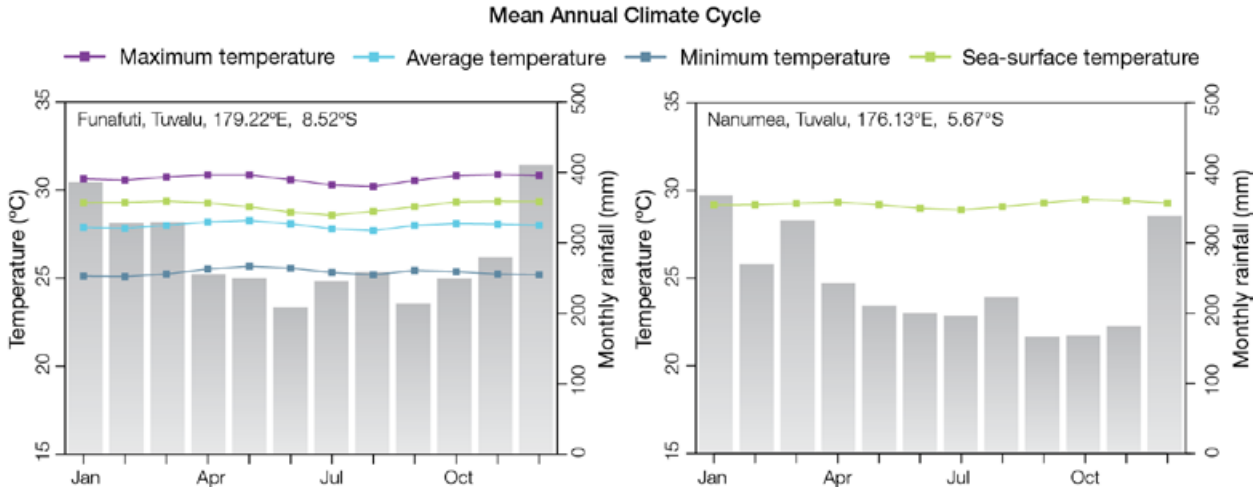

Figure 15.2: Mean annual cycle of rainfall (grey bars) and daily maximum, minimum and mean air temperatures at Funafuti (left) and Nanumea (right – rainfall only), and local sea-surface temperatures derived from the HadISST dataset (Volume 1, Table 2.3).

15.5 Climate Variability

High year-to-year variability in rainfall is observed in Tuvalu, mostly due to the impact of the El Niño-Southern Oscillation (ENSO; Figure 15.4). In the wettest years Funafuti receives about twice as much rainfall as in the driest years, while in Nanumea this can be as much as five times more. In an El Niño year, the SPCZ tends to move to the north-east over Tuvalu and so rainfall is higher. This impact is mainly seen in the dry season at Funafuti, but further north at Nanumea the effect is even stronger, especially in the wet season (Tables 15.1 and 15.2). At Nanumea the SPCZ tends to move over the island in El Niño years and away to the south-west in La Niña years, bringing severe drought. Considerable decadal variability is also evident in rainfall in Tuvalu, but the correlations with the Interdecadal Pacific Oscillation show only a weak relationship with wet-season rainfall in Nanumea.

In contrast to rainfall, interannual variability in average surface air temperatures is very small in Funafuti, although ENSO has some impact on air temperatures. Minimum temperatures are higher during El Niño years and lower in La Niña years, as are maximum air temperatures during the wet season. The influence is likely due to the warmer ocean temperatures around Tuvalu in El Niño years.

ENSO Modoki (Volume 1, Section 3.4.1) has a significant impact on rainfall and temperatures, but this impact is generally weaker than canonical El Niño and La Niña events. However, the impacts of ENSO Modoki events on maximum air temperatures and wet season minimum air temperatures are stronger. They also affect rainfall during the dry season in Funafuti and the wet season in Nanumea.

Table 15.1: Correlation coefficients between indices of key large-scale patterns of climate variability and minimum and maximum temperatures (Tmin and Tmax) and rainfall at Funafuti. Only correlation coefficients that are statistically significant at the 95% level are shown.

Climate feature/index		Dry season (May-October)			Wet season (November-April)		
		Tmin	Tmax	Rain	Tmin	Tmax	Rain
ENSO	Niño3.4	0.25		0.41	0.35	0.39	
	Southern Oscillation Index	-0.25		-0.47	-0.29		
Interdecadal Pacific Oscillation Index							
ENSO Modoki Index			0.28	0.27	0.41	0.60	
Number of years of data		64	64	76	63	63	77

Table 15.2: Correlation coefficients between indices of key large-scale patterns of climate variability and minimum and maximum temperatures (Tmin and Tmax) and rainfall at Nanumea. Only correlation coefficients that are statistically significant at the 95% level are shown.

Climate feature/index		Dry season (May-October)	Wet season (November-April)
		Rain	Rain
ENSO	Niño3.4	0.59	0.80
	Southern Oscillation Index	-0.58	-0.83
Interdecadal Pacific Oscillation Index			0.25
ENSO Modoki Index			0.50
Number of years of data		64	64

Training in *Pacific Climate Futures*, Funafuti

15.6 Observed Trends

15.6.1 Air Temperature

Warming trends are evident in both annual and seasonal mean air temperatures at Funafuti from 1950 (Figure 15.3 and Table 15.3), with the strongest trend in dry season mean air temperature (+0.24°C per decade). Trends in minimum air temperatures are slightly stronger than those calculated for maximum air temperatures.

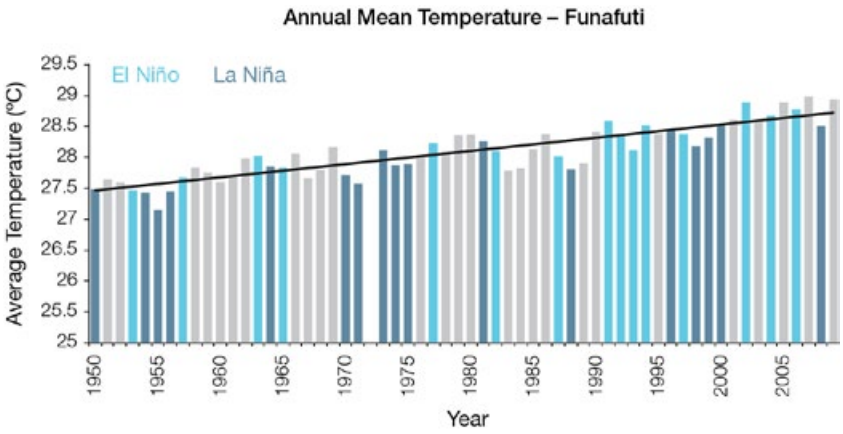

Figure 15.3: Annual mean air temperature at Funafuti. Light blue, dark blue and grey bars denote El Niño, La Niña and neutral years respectively.

15.6.2 Rainfall

Annual and seasonal rainfall trends for Funafuti and Nanumea for the period 1950—2009 are not statistically significant (Table 15.3 and Figure 15.4).

15.6.3 Extreme Events

The tropical cyclone season in Tuvalu is from November to April. Occurrences outside this period are rare. The tropical cyclone archive for the Southern Hemisphere indicates that between the 1969/70 and 2006/07 cyclone seasons the centre of 33 tropical cyclones passed within approximately 400 km of Funafuti. This represents an average of eight cyclones per decade. Tropical cyclones were most frequent in El Niño years (12 cyclones per decade) and least frequent in La Niña years (four cyclones per decade). The ENSO-neutral season average is six cyclones per decade. The interannual variability in the number of tropical cyclones in the vicinity of Funafuti is large, ranging from zero in some seasons to three in the 1997/98 season (Figure 15.5). This high variability makes it difficult to identify any long-term trends in frequency.

Tropical cyclones and spring tides are the main extreme events that affect Funafuti. In addition to high winds and rainfall, tropical cyclones also generate storm surge and swell, resulting in land inundation. This results in agricultural losses (especially taro) and damage to buildings and roads along the coast.

Table 15.3: Annual and seasonal trends in maximum, minimum and mean air temperature (Tmax, Tmin and Tmean) and rainfall at Funafuti and Nanumea for 1950–2009. Asterisks indicate significance at the 95% level. Persistence is taken into account in the assessment of significance as in Power and Kociuba (in press). The statistical significance of the air temperature trends is not assessed.

	Funafuti Tmax (°C per 10 yrs)	Funafuti Tmin (°C per 10 yrs)	Funafuti Tmean (°C per 10 yrs)	Funafuti Rain (mm per 10 yrs)	Nanumea Rain (mm per 10 yrs)
Annual	+0.21	+0.22	+0.21	-45	-2
Wet season	+0.18	+0.20	+0.19	-37	-4
Dry season	+0.24	+0.25	+0.24	-13	+1

15.6.4 Sea-Surface Temperature

Water temperatures around Tuvalu have risen gradually since the 1950s with the rate increasing over time. Since the 1970s the rate of warming has been approximately 0.13°C per decade. Figure 15.8 shows the 1950–2000 sea-surface temperature changes (relative to a reference year of 1990) from three different large-scale sea surface temperature datasets (HadSST2, ERSST and Kaplan Extended SST V2; Volume 1, Table 2.3). At these regional scales, natural variability may play a large role in determining sea-surface temperature in the region making it difficult to identify any long-term trends.

15.6.5 Ocean Acidification

Based on the large-scale distribution of coral reefs across the Pacific and the seawater chemistry, Guinotte et al. (2003) suggested that seawater aragonite saturation states above 4 were optimal for coral growth and for the development of healthy reef ecosystems, with values from 3.5 to 4 adequate for coral growth, and values between 3 and 3.5, marginal. Coral reef ecosystems were not found at seawater aragonite saturation states below 3 and these conditions were classified as extremely marginal for supporting coral growth.

In the Tuvalu region, the aragonite saturation state has declined from about 4.5 in the late 18th century to an observed value of about 4.0 ± 0.1 by 2000.

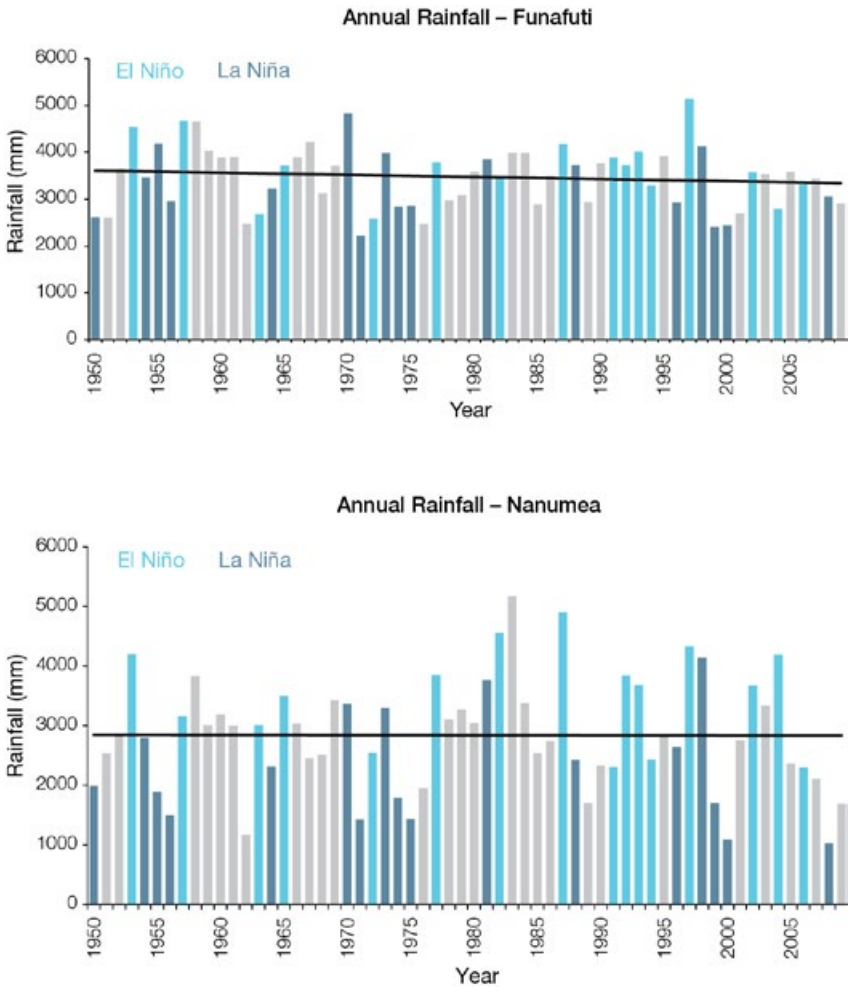

Figure 15.4: Annual rainfall for Funafuti (top) and Nanumea (bottom). Light blue, dark blue and grey bars denote El Niño, La Niña and neutral years respectively.

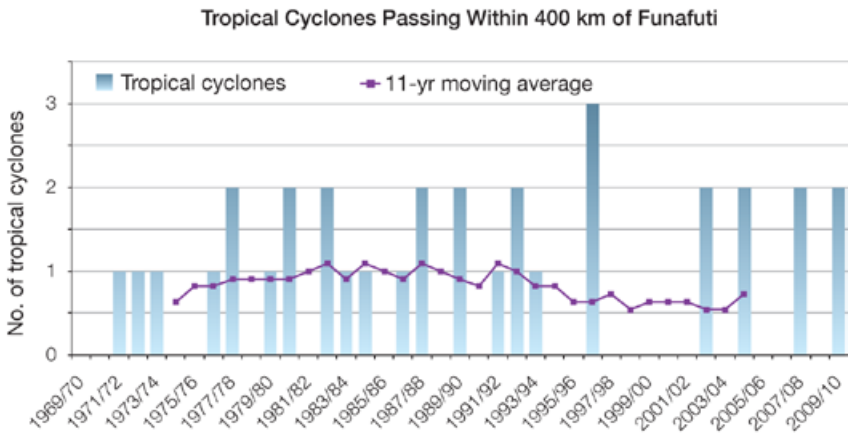

Figure 15.5: Tropical cyclones passing within 400 km of Funafuti per season. The 11-year moving average is in purple.

15.6.6 Sea Level

Monthly averages of the historical tide gauge, satellite (since 1993) and gridded sea-level (since 1950) data agree well after 1993 and indicate interannual variability in sea levels of about 26 cm (estimated 5–95% range) after removal of the seasonal cycle (Figure 15.10). The sea-level rise near Tuvalu measured by satellite altimeters (Figure 15.6) since 1993 is about 5 mm per year, larger than the global average of 3.2 ± 0.4 mm per year. This rise is partly linked to a pattern related to climate variability from year to year and decade to decade (Figure 15.10).

15.6.7 Extreme Sea-Level Events

The annual climatology of the highest daily sea levels has been evaluated from hourly measurements by tide gauges at Funafuti (Figure 15.7). Tides and short-term sea-level fluctuations create a tendency for highest annual water levels to occur during February through March. This is consistent with the timing of most of the top 10 highest sea levels recorded which all occur during these months. During La Niña years, there is a tendency for sea levels to be higher due to warmer ocean temperatures which influence the seasonal contributions (Volume 1, Section 3.6.3 and Figures 3.20 and 3.21) whereas short-term contributions to sea level due to the influence of weather events tend to be lower than the all-year averages. In other words, the seasonal and short-term influences appear to exert opposite influences on sea-level extremes. During El Niño, the seasonal contribution to extreme sea levels is lower whereas the short-term contribution is largely unchanged from the all-year averages. The top 10 events all occurred from February to April; six during ENSO-neutral years, three during La Niña years and one during El Niño. This suggests that tides exert a strong influence on the occurrence of sea-level extremes where as the influence of the ENSO cycle is less important.

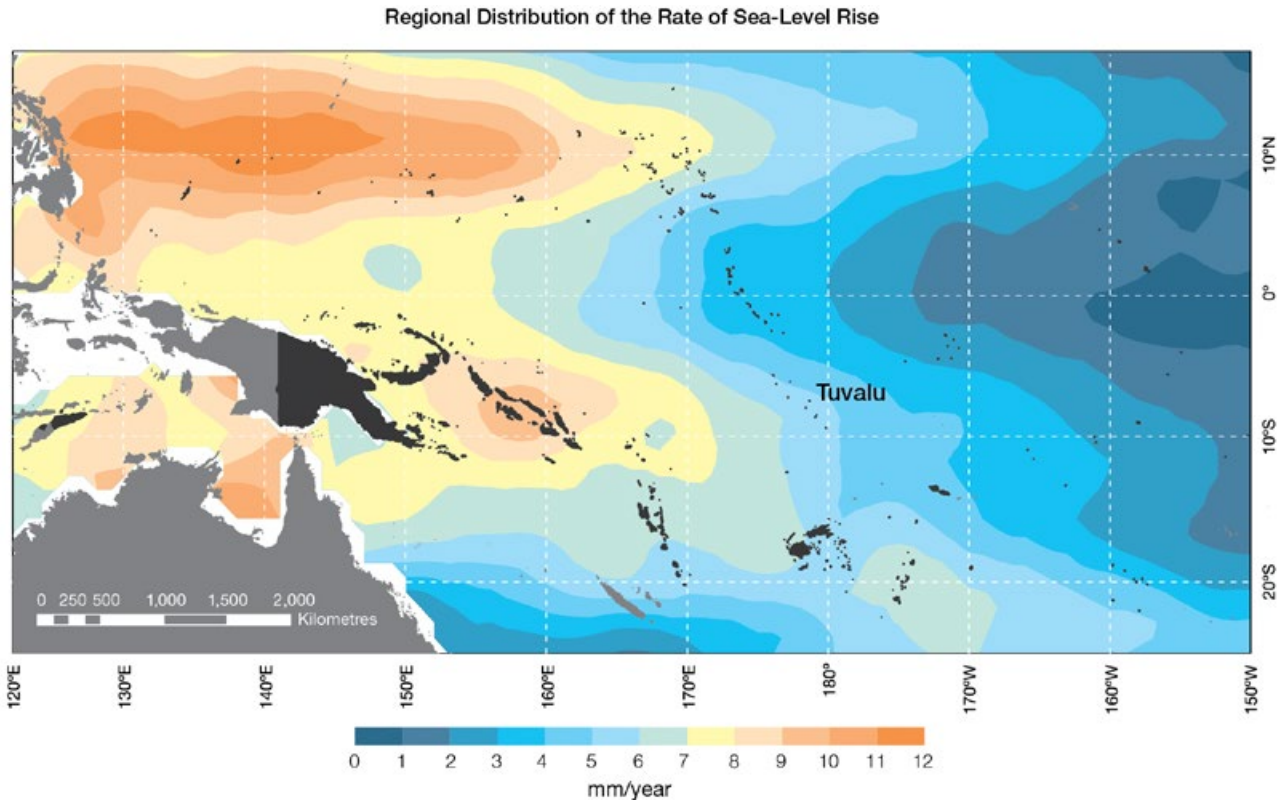

Figure 15.6: The regional distribution of the rate of sea-level rise measured by satellite altimeters from January 1993 to December 2010, with the location of Tuvalu indicated. Further detail about regional distribution of sea-level rise is provided in Volume 1, Section 3.6.3.2.

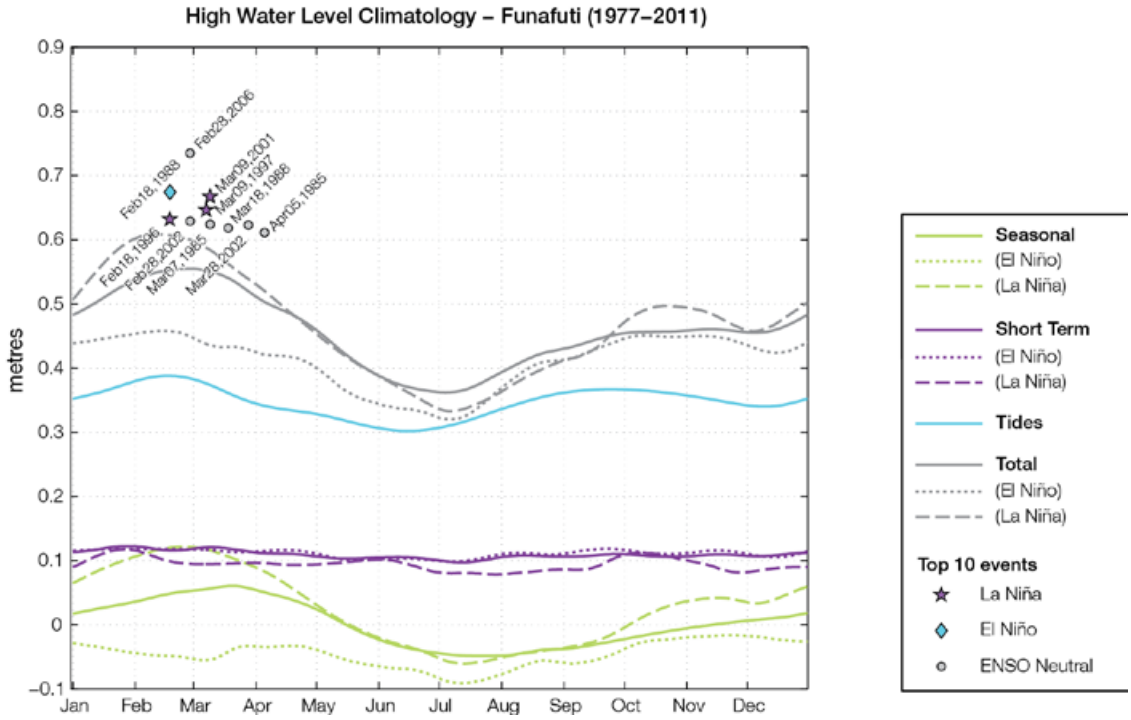

Figure 15.7: The annual cycle of high waters relative to Mean Higher High Water (MHHW) due to tides, short-term fluctuations (most likely associated with storms) and seasonal variations for Tuvalu. The tides and short-term fluctuations are respectively the 95% exceedence of the astronomical high tides relative to MHHW and short-term sea level fluctuations. Components computed only for El Niño and La Niña months are shown by dotted and dashed lines, and grey lines are the sum of the tide, short-term and seasonal components. The 10 highest sea-level events in the record relative to MHWW are shown, and coded to indicate the phase of ENSO at the time of the extreme event.

15.7 Climate Projections

Climate projections have been derived from up to 18 global climate models from the CMIP3 database, for up to three emissions scenarios (B1 (low), A1B (medium) and A2 (high)) and three 20-year periods (centred on 2030, 2055 and 2090, relative to 1990). These models were selected based on their ability to reproduce important features of the current climate (Volume 1, Section 5.2.3), so projections from each of the models are plausible representations of the future climate. This means there is not one single projected future for Tuvalu, but rather a range of possible futures. The full range of these futures is discussed in the following sections.

These projections do not represent a value specific to any actual location, such as a town in Tuvalu. Instead, they refer to an average change over the broad geographic region encompassing the islands of Tuvalu and the surrounding ocean (Figure 1.1 shows the regional boundaries). Section 1.7 provides important information about understanding climate model projections.

15.7.1 Temperature

Surface air temperature and sea-surface temperature are projected to continue to increase over the course of the 21st century. There is *very high* confidence in this direction of change because:

- Warming is physically consistent with rising greenhouse gas concentrations.
- All CMIP3 models agree on this direction of change.

The majority of CMIP3 models simulate a slight increase (<1°C) in annual and seasonal mean temperature by 2030, however by 2090 under the A2 (high) emissions scenario temperature increases of greater than 2.5°C are simulated by almost all models (Table 15.4). Given the close relationship between surface air temperature and sea-surface temperature, a similar (or slightly weaker) rate of warming is projected for the surface ocean (Figure 15.8). There is *high* confidence in this range and distribution of possible futures because:

- There is generally close agreement between modelled and observed temperature trends over the past 50 years in the vicinity of Tuvalu, although observational records are limited (Figure 15.8).

Interannual variability in surface air temperature and sea-surface temperature over Tuvalu is strongly influenced by ENSO in the current climate (Section 15.5). As there is no consistency in projections of future ENSO activity (Volume 1, Section 6.4.1) it is not possible to determine whether interannual variability in temperature will change in the future. However, ENSO is expected to continue to be an important source of variability for the region.

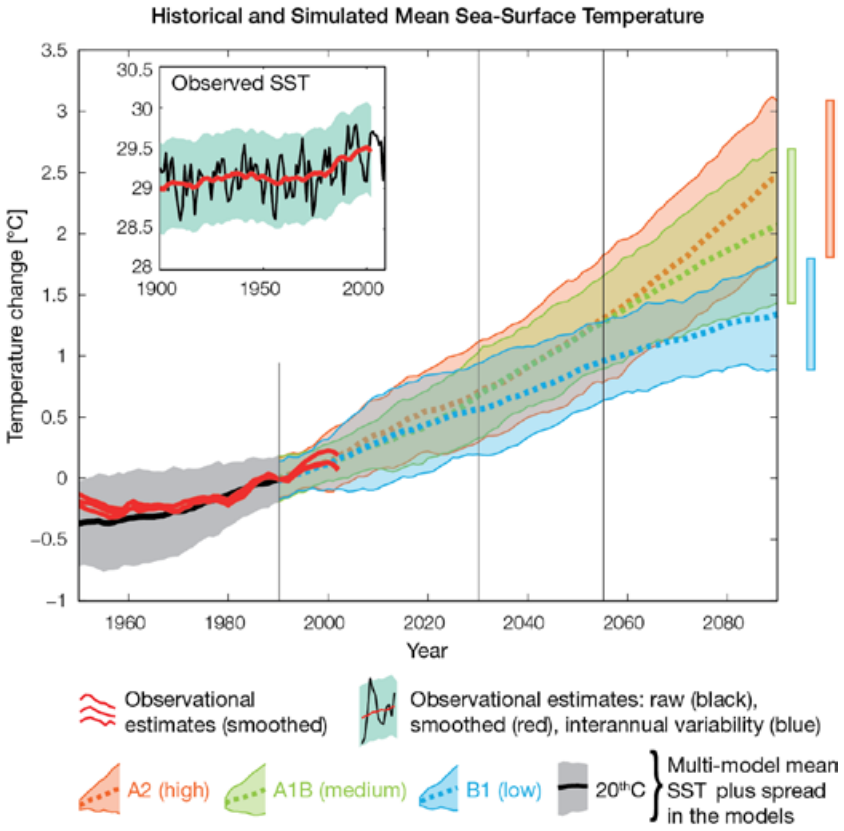

Figure 15.8: Historical climate (from 1950 onwards) and simulated historical and future climate for annual mean sea-surface temperature (SST) in the region surrounding Tuvalu, for the CMIP3 models. Shading represents approximately 95% of the range of model projections (twice the inter-model standard deviation), while the solid lines represent the smoothed (20-year running average) multi-model mean temperature. Projections are calculated relative to the 1980–1999 period (which is why there is a decline in the inter-model standard deviation around 1990). Observational estimates in the main figure (red lines) are derived from the HadSST2, ERSST and Kaplan Extended SST V2 datasets (Volume 1, Section 2.2.2). Annual average (black) and 20-year running average (red) HadSST2 data is also shown inset.

15.7.2 Rainfall

Wet season (November-April), dry season (May-October) and annual average rainfall are projected to increase over the course of the 21st century. There is *high* confidence in this direction of change because:

- Physical arguments indicate that rainfall will increase in the equatorial Pacific in a warmer climate (IPCC, 2007; Volume 1, Section 6.4.3).
- Almost all of the CMIP3 models agree on this direction of change by 2090.

The majority of CMIP3 models simulate little change (-5% to 5%) in wet season, dry season and annual mean rainfall by 2030, however by 2090 the majority simulate an increase (>5%), with up to a third simulating a large increase (> 5%) under the A2 (high) emissions scenario (Table 15.4). There is *moderate* confidence in this range and distribution of possible futures because:

- In simulations of the current climate, the CMIP3 models broadly capture the influence of the West Pacific Monsoon and the South Pacific Convergence Zone on the rainfall of Tuvalu (Volume 1, Section 5.2.3), although most models produce monsoon westerly winds that do not extend far enough east into the Pacific basin.
- The CMIP3 models are unable to resolve many of the physical processes involved in producing rainfall. As a consequence, they do not simulate rainfall as well as other variables such as temperature (Volume 1, Chapter 5).

Interannual variability in rainfall over Tuvalu is strongly influenced by ENSO in the current climate (Section 15.5). As there is no consistency in projections of future ENSO activity (Volume 1, Section 6.4.1) it is not possible to determine whether interannual variability in rainfall will change in the future.

15.7.3 Extremes

Temperature

The intensity and frequency of days of extreme heat are projected to increase over the course of the 21st century. There is *very high* confidence in this direction of change because:

- An increase in the intensity and frequency of days of extreme heat is physically consistent with rising greenhouse gas concentrations.
- All CMIP3 models agree on the direction of change for both intensity and frequency.

The majority of CMIP3 models simulate an increase of approximately 1°C in the temperature experienced on the 1-in-20-year hot day by 2055 under the B1 (low) emissions scenario, with an increase of over 2.5°C simulated by the majority of models by 2090 under the A2 (high) emissions scenario (Table 15.4). There is *low* confidence in this range and distribution of possible futures because:

- In simulations of the current climate, the CMIP3 models tend to underestimate the intensity and frequency of days of extreme heat (Volume 1, Section 5.2.4).
- Smaller increases in the frequency of days of extreme heat are projected by the CCAM 60 km simulations.

Rainfall

The intensity and frequency of days of extreme rainfall are projected to increase over the course of the 21st century. There is *high* confidence in this direction of change because:

- An increase in the frequency and intensity of extreme rainfall is consistent with larger-scale projections, based on the physical argument that the atmosphere is able to hold more water vapour in a warmer climate (Allen and Ingram, 2002; IPCC, 2007). It is also consistent with physical arguments which indicate that rainfall will increase in the deep tropical Pacific in a warmer climate (IPCC, 2007; Volume 1, Section 6.4.3).
- Almost all of the CMIP3 models agree on this direction of change for both intensity and frequency.

The majority of CMIP3 models simulate an increase of at least 20 mm in the amount of rain received on the 1-in-20-year wet day by 2055 under the B1 (low) emissions scenario, with an increase of at least 35 mm simulated by 2090 under the A2 (high) emissions scenario. The majority of models project that the current 1-in-20-year extreme rainfall event will occur, on average, four to five times per 20-year period by 2055 under the B1 (low) emissions scenario and six to seven times per 20-year period by 2090 under the A2 (high) emissions scenario. There is *low* confidence in this range and distribution of possible futures because:

- In simulations of the current climate, the CMIP3 models tend to underestimate the intensity and frequency of extreme rainfall (Volume 1, Section 5.2.4).
- The CMIP3 models are unable to resolve many of the physical processes involved in producing extreme rainfall.

Drought

The incidence of drought is projected to decrease over the course of the 21st century. There is *moderate* confidence in this direction of change because:

- A decrease in drought is consistent with projections of increased rainfall (Section 15.7.2).
- The majority of models agree on this direction of change for most drought categories.

The majority of CMIP3 models project that mild drought will occur approximately eight to nine times every 20 years in 2030 under all emissions scenarios, decreasing to six to seven times by 2090. The frequency of moderate and severe drought is projected to remain approximately stable from 2030 throughout the 21st century at once to twice and once every 20 years, respectively.

There is *low* confidence in this range and distribution of possible futures because:

- There is only moderate confidence in the range of rainfall projections (Section 15.7.2), which directly influences projections of future drought conditions.

Tropical Cyclones

Tropical cyclone numbers are projected to decline in the south-east Pacific Ocean basin (0–40ºS, 170ºE–130ºW) over the course of the 21st century. There is *moderate* confidence in this direction of change because:

- Many studies suggest a decline in tropical cyclone frequency globally (Knutson et al., 2010).
- Tropical cyclone numbers decline in the south-east Pacific Ocean in the majority assessment techniques.

Based on the direct detection methodologies (Curvature Vorticity Parameter (CVP) and the CSIRO Direct Detection Scheme (CDD) described in Volume 1, Section 4.8.2), 65% of projections show no change or a decrease in tropical cyclone formation when applied to the CMIP3 climate models for which suitable output is available. When these techniques are applied to CCAM, 100% of projections show a decrease in tropical cyclone formation. In addition, the Genesis Potential Index (GPI) empirical technique suggests that conditions for tropical cyclone formation will become less favourable in the south-east Pacific Ocean basin, for all analysed CMIP3 models. There is moderate confidence in this range and distribution of possible futures because in simulations of the current climate, the CVP, CDD and GPI methods capture the frequency of tropical cyclone activity reasonably well (Volume 1, Section 5.4).

Despite this projected reduction in total cyclone numbers, five of the six CCAM 60 km simulations show an increase in the proportion of the most severe cyclones. Most models also indicate a reduction in tropical cyclone wind hazard north of 20ºS latitude and regions of increased hazard south of 20ºS latitude. This increase in wind hazard coincides with a poleward shift in the latitude at which tropical cyclones are most intense.

15.7.4 Ocean Acidification

The acidification of the ocean will continue to increase over the course of the 21st century. There is *very high* confidence in this projection as the rate of ocean acidification is driven primarily by the increasing oceanic uptake of carbon dioxide, in response to rising atmospheric carbon dioxide concentrations.

Projections from all analysed CMIP3 models indicate that the annual maximum aragonite saturation state will reach values below 3.5 by about 2060 and continue to decline thereafter (Figure 15.9; Table 15.4). There is *moderate* confidence in this range and distribution of possible futures because the projections are based on climate models without an explicit representation of the carbon cycle and with relatively low resolution and known regional biases.

The impact of acidification change on the health of reef ecosystems is likely to be compounded by other stressors including coral bleaching, storm damage and fishing pressure.

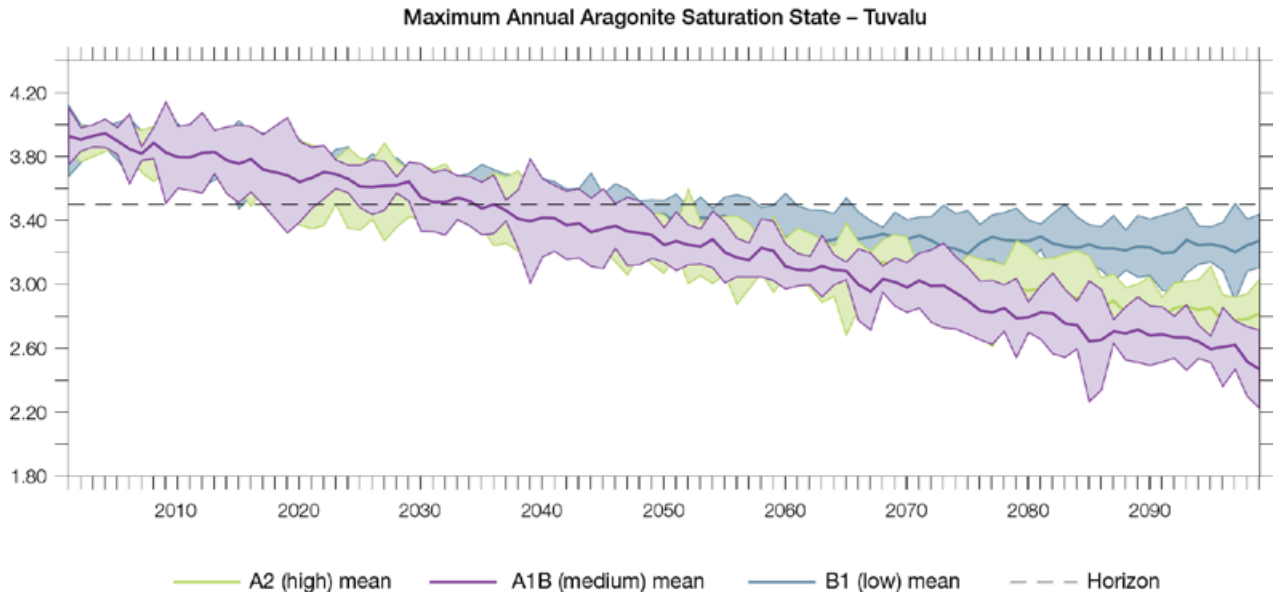

Figure 15.9: Multi-model projections, and their associated uncertainty (shaded area represents two standard deviations), of the maximum annual aragonite saturation state in the sea surface waters of the Tuvalu region under the different emissions scenarios. The dashed black line represents an aragonite saturation state of 3.5.

15.7.5 Sea Level

Mean sea level is projected to continue to rise over the course of the 21st century. There is *very high* confidence in this direction of change because:

- Sea-level rise is a physically consistent response to increasing ocean and atmospheric temperatures, due to thermal expansion of the water and the melting of glaciers and ice caps.
- Projections arising from all CMIP3 models agree on this direction of change.

The CMIP3 models simulate a rise of between approximately 5–15 cm by 2030, with increases of 20–60 cm indicated by 2090 under the higher-emissions scenarios (i.e. A2 (high) and A1B (medium); Figure 15.10; Table 15.4). There is *moderate* confidence in this range and distribution of possible futures because:

- There is significant uncertainty surrounding ice-sheet contributions to sea-level rise and a rise larger than that projected above cannot be excluded (Meehl et al., 2007b). However, understanding of the processes is currently too limited to provide a best estimate or an upper bound (IPCC, 2007).
- Globally, since the early 1990s, sea level has been rising near the upper end of the above projections. During the 21st century, some studies (using semi-empirical models) project faster rates of sea-level rise.

Interannual variability of sea level will lead to periods of lower and higher regional sea levels. In the past, this interannual variability has been about 26 cm (5–95% range, after removal of the seasonal cycle; dashed lines in Figure 15.10 (a)) and it is likely that a similar range will continue through the 21st century. In addition, winds and waves associated with weather phenomena will continue to lead to extreme sea-level events.

In addition to the regional variations in sea level associated with ocean and mass changes, there are ongoing changes in relative sea level associated with changes in surface loading over the last glacial cycle (glacial isostatic adjustment) and local tectonic motions. The glacial isostatic motions are relatively small for the PCCSP region.

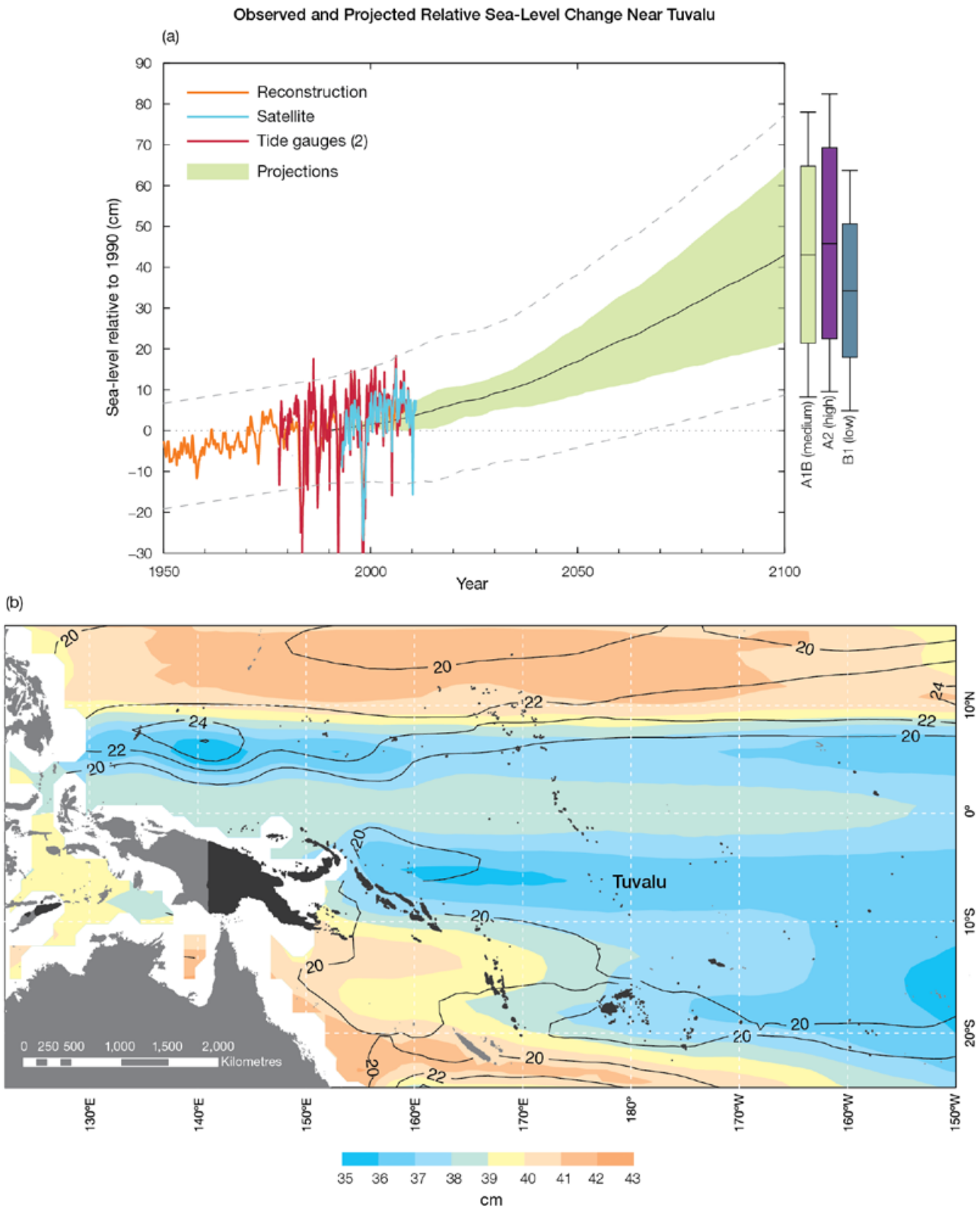

Figure 15.10: Observed and projected relative sea-level change near Tuvalu. (a) The observed in situ relative sea-level records are indicated in red, with the satellite record (since 1993) in light blue. The gridded sea level at Tuvalu (since 1950, from Church and White (in press)) is shown in orange. The projections for the A1B (medium) emissions scenario (5–95% uncertainty range) are shown by the green shaded region from 1990–2100. The range of projections for the B1 (low), A1B (medium) and A2 (high) emissions scenarios by 2100 are also shown by the bars on the right. The dashed lines are an estimate of interannual variability in sea level (5–95% range about the long-term trends) and indicate that individual monthly averages of sea level can be above or below longer-term averages. (b) The projections (in cm) for the A1B (medium) emissions scenario in the Tuvalu region for the average over 2081–2100 relative to 1981–2000 are indicated by the shading, with the estimated uncertainty in the projections indicated by the contours (in cm).

15.7.6 Projections Summary

The projections presented in Section 15.7 are summarised in Table 15.4. For detailed information regarding the various uncertainties associated with the table values, refer to the preceding text in Sections 15.7 and 1.7, in addition to Chapters 5 and 6 in Volume 1. When interpreting the differences between projections for the B1 (low), A1B (medium) and A2 (high) emissions scenarios, it is also important to consider the emissions pathways associated with each scenario (Volume 1, Figure 4.1) and the fact that a slightly different subset of models was available for each (Volume 1, Appendix 1).

Table 15.4: Projected change in the annual and seasonal mean climate for Tuvalu, under the B1 (low; blue), A1B (medium; green) and A2 (high; purple) emissions scenarios. Projections are given for three 20-year periods centred on 2030 (2020–2039), 2055 (2046–2065) and 2090 (2080–2099), relative to 1990 (1980–1999). Values represent the multi-model mean change ± twice the inter-model standard deviation (representing approximately 95% of the range of model projections), except for sea level where the estimated mean change and the 5–95% range are given (as they are derived directly from the Intergovernmental Panel on Climate Change Fourth Assessment Report values). The confidence (Section 1.7.2) associated with the range and distribution of the projections is also given (indicated by the standard deviation and multi-model mean, respectively). See Volume 1, Appendix 1 for a complete listing of CMIP3 models used to derive these projections.

Variable	Season	2030	2055	2090	Confidence
Surface air temperature (°C)	Annual	+0.7 ± 0.4 +0.8 ± 0.4 +0.7 ± 0.3	+1.1 ± 0.4 +1.5 ± 0.5 +1.4 ± 0.4	+1.5 ± 0.6 +2.3 ± 0.8 +2.7 ± 0.6	High
Maximum temperature (°C)	1-in-20-year event	N/A	+1.0 ± 0.6 +1.5 ± 0.6 +1.5 ± 0.5	+1.4 ± 0.7 +2.1 ± 1.1 +2.7 ± 1.3	Low
Minimum temperature (°C)	1-in-20-year event	N/A	+1.2 ± 1.8 +1.5 ± 2.0 +1.5 ± 1.8	+1.6 ± 1.8 +2.2 ± 2.0 +2.4 ± 1.9	Low
Total rainfall (%)*	Annual	+3 ± 8 +3 ± 8 +4 ± 8	+7 ± 11 +7 ± 10 +7 ± 12	+7 ± 12 +12 ± 14 +11 ± 18	Moderate
Wet season rainfall (%)*	November-April	+3 ± 10 +3 ± 9 +4 ± 8	+7 ± 9 +6 ± 11 +6 ± 10	+7 ± 11 +11 ± 14 +11 ± 16	Moderate
Dry season rainfall (%)*	May-October	+3 ± 10 +4 ± 11 +5 ± 13	+7 ± 16 +7 ± 16 +8 ± 19	+8 ± 18 +12 ± 23 +12 ± 26	Moderate
Sea-surface temperature (°C)	Annual	+0.6 ± 0.4 +0.7 ± 0.3 +0.7 ± 0.4	+1.0 ± 0.3 +1.3 ± 0.4 +1.3 ± 0.5	+1.3 ± 0.5 +2.1 ± 0.6 +2.5 ± 0.6	High
Aragonite saturation state (Ωar)	Annual maximum	+3.6 ± 0.1 +3.5 ± 0.2 +3.5 ± 0.2	+3.3 ± 0.1 +3.2 ± 0.2 +3.2 ± 0.1	+3.2 ± 0.2 +2.8 ± 0.2 +2.6 ± 0.2	Moderate
Mean sea level (cm)	Annual	+9 (4–14) +9 (5–14) +9 (4–14)	+17 (9–25) +19 (10–29) +19 (9–28)	+31 (16–45) +37 (19–56) +39 (19–58)	Moderate

*The MIROC3.2(medres) and MIROC3.2(hires) models were eliminated in calculating the rainfall projections, due to their inability to accurately simulate present-day activity of the South Pacific Convergence Zone and/or the West Pacific Monsoon (Volume 1, Section 5.5.1).